Applied Thermal Engineering 158 (2019) 113809

Contents lists available at ScienceDirect

Applied Thermal Engineering

journal homepage: www.elsevier.com/locate/apthermeng

Research Paper

Dynamic modeling of room temperature and thermodynamic efficiency for direct expansion air conditioning systems using Bayesian neural network

Sholahudin[a,*], Keisuke Ohno[b], Niccolo Giannetti[c], Seiichi Yamaguchi[a,b], Kiyoshi Saito[a,b]

[a] Department of Applied Mechanics and Aerospace Engineering, Waseda University, 3-4-1 Okubo, Shinjuku-ku, Tokyo 169-8555, Japan
[b] Interdisciplinary Institute for Thermal Energy Conversion Engineering and Mathematics, Waseda University, 3-4-1 Okubo, Shinjuku-ku, Tokyo 169-8555, Japan
[c] Waseda Institute for Advanced Study, Waseda University, 1-6-1 Nishiwaseda, Shinjuku-ku, Tokyo 169-8050, Japan

ARTICLE INFO

Keywords:
Exergy destruction
Thermal comfort
Dynamic modeling
Air conditioning

ABSTRACT

In this paper, dynamic performance identification for a direct expansion (DX) air conditioning (AC) system is proposed using Bayesian artificial neural network (ANN). The input and output datasets are generated by a dedicated AC simulator by varying the compressor speed in various signal amplitudes and including dynamic cooling load and ambient temperature. The exergy destruction, which represents the work potential losses in the system and room temperature indicating the thermal comfort are selected as the output variables. The key parameters of an ANN model, including the number of neurons and tapped delay lines, are optimized to improve the prediction accuracy. The results show that the dynamic response of the exergy destruction and room temperature can be predicted accurately by the optimized ANN model using three neurons, a Bayesian regularization algorithm, five delayed inputs for the compressor speed and room temperature, and six delayed inputs for the cooling load and ambient temperature. The validation of the multi-step-ahead prediction showed satisfying results with respect to the root mean squared errors (RMSEs) and coefficient of variations (CVs) of the room temperature (RMSE: 0.18 °C and CV: 0.85%) and exergy destruction (RMSE: 1.79 W and CV: 0.4%). Accordingly, the identification of the AC system behavior presented in this paper could be further implemented to control the DX AC system operation to achieve a desired thermal comfort with low exergy destruction.

1. Introduction

In recent years, many researchers have paid significant attention to energy issues. This is because the availability of fossil energy resources is limited, while energy demand is increasing due to the increase in the population and industry developments. In addition, high energy usage leads to greater CO_2 emission, which is potentially harmful for the environment [1]. In Europe, 40% of the total energy usage is consumed by the building sector [2]. One of the big contributors to the building energy consumption is heating, ventilating, and air conditioning (HVAC) system. On the one hand, in terms of the standard indexes such as the coefficient of performance (COP) and annual performance factor (APF), the AC system technologies that include vapor compression [3], sorption [4–6], ejection [7], and inverse Brayton [8,9] have reached performance levels that are close to the theoretical limitations. On the other hand, the steady conditions at which these indexes are measured are very different from the operative conditions encountered during the actual operation. Therefore, the seasonal performance of operative systems is in fact far from their nominal efficiency [10]. Hence, developing advanced modeling and control strategies, which consider the real operation of these systems since an early pre-design stage, represents an opportunity to significantly reduce the annual building energy consumption.

Vapor compression DX AC systems have been widely used in many residential buildings. This technology is well suited for small to medium building sizes because it exhibits a high nominal efficiency, flexibility in installation, and ease of maintenance [11]. However, the installed system control strategy is typically designated to achieve thermal comfort only, without taking into account the system efficiency. Ideally, the AC system should be operated to meet the desired thermal comfort while maintaining the system efficiency. Under this viewpoint, advanced identification procedures of the dynamic behavior of DX AC systems are necessary to reliably evaluate the system performance. This is required as the first effort to determine proper control strategy for the system. Theoretically, modeling of the dynamic behavior of DX AC systems is very complex; the system is composed of several components, which are connected to each other and result in nonlinear dynamic correlations between the input and output.

* Corresponding author.
E-mail address: sholahudin@fuji.waseda.jp (Sholahudin).

https://doi.org/10.1016/j.applthermaleng.2019.113809
Received 25 December 2018; Received in revised form 23 April 2019; Accepted 22 May 2019
Available online 23 May 2019
1359-4311/

Nomenclature

Notation

A_i	alternative
b	bias coefficient
C_p	heat capacity (J/kg K)
C_j	attribute
c_1, c_2	weighting parameter
D	training data sets
E_D	sum of squared error
E_W	sum of squared weight
$\dot{E}x$	specific exergy (W)
$\dot{E}x_{dest}$	exergy destruction (W)
f	transfer function
h	specific enthalpy (kJ/kg)
J_{reg}	objective function
k	number of weight and bias
M	network architecture
$\dot{m}$	mass flow rate (kg/s)
N	compressor speed
n	output from hidden layer
n_a	number of alternatives
n_p	number of attribute
Net_{comp}	network complexity
Q	energy transfer (W)
r_{ij}	normalized score
s	specific entropy (J/K)
T	temperature (°C)
t_j	calculated output
u	ANN input
V	volume (m^3)
V_i	preference value
$\dot{W}_{out}$	work (W)
w_j	attribute weight
w	weight coefficient
	attribute score
x	vector of weight and bias
y_j	predicted output
y	ANN output

Greek

α, β	regularization parameter
ρ	density (kg/m^3)

Subscript

A	ambient
C	condenser
E	evaporator
i	evaporator surrounding
l	load
m	refrigeration state
o	condenser surrounding
R	room
0	dead state

Dynamic modeling of a DX AC system has been successfully proposed to analyze the response of exergy destruction [12]; room temperature [13]; evaporator and condenser air outlet temperatures [14]; and condensing, evaporating, and superheat temperatures [15], using physical models derived from the mass continuity, energy conservation, and thermodynamic theory. This method is considered to have a high generalization capability [16]. However, it requires detailed information on the system characteristics, and a high computational effort is required to solve nonlinear systems of large numbers of differential or algebraic equations [17]. Owing to the simplifying assumptions necessarily introduced, the results may be affected by large deviations if carried out outside their range of validity. Therefore, the implementation of a physical-based model for dynamic modeling with adequate accuracy for predictive control is very challenging. As an alternative solution, a data-driven model using an artificial neural network (ANN) can be considered to establish the system identification of an AC system. This method is simpler and faster compared with physical models since it can achieve accurate predictions with a limited set of input parameters. In this case, the ANN could be trained with data obtained from numerical simulations or from extensive experimental investigation, as well as from a combination of these two methods.

In the last decade, ANN has been introduced to predict the performance of an AC system for absorption [18] and vapor compression [19–21] systems. Tian et al. [19] optimized the ANN structure to predict the mass flow of refrigerant, condenser heat rejection, refrigeration capacity, and compressor energy consumption in the steady state condition for an electric vehicle AC system. The results show that the ANN model with thirteen neurons provides the most accurate prediction. Kamar et al. [20] conducted similar research, using the ANN model to predict the performance of a vehicle AC system. The ANN configuration was developed to predict the one-step ahead output of the compressor energy consumption, cooling effect, and COP. The results show that the optimized ANN model achieved a high prediction accuracy with a correlation coefficient close to unity. Munoz et al. [21] introduced the ANN to predict and control indoor air temperature and humidity. The data sets were generated by operating compressor speed and fan for air distribution in the experimental rig. The results show that the developed ANN has a good performance in modeling the dynamic behavior of the temperature and humidity.

According to the related literature, previous works [11,17,21] developed ANN models for the prediction of the thermal comfort parameters without considering the thermodynamic performance, dynamic cooling load, and ambient temperature. The ANN model introduced in Ref. [11] was developed for online training applications to handle the disturbances from the dynamic cooling load and ambient temperature. The online training approach is reliable if all of the input and output data is easy to measure during the real time operation [11]. However, it is hard to apply for exergy destruction due to the required calculation parameters, such as the pressure, temperature, and refrigerant mass flow rate are complicated to obtain. In addition, the refrigerant properties including the enthalpy and entropy should be provided. Consequently, it is to be mentioned that the ANN model for exergy based optimal control must be trained offline. Moreover, the exergy analyses of the vapor compression system are mostly performed in the steady state condition which is only applicable to find the optimum system performance at the design stage [22–26]. To address the challenge of obtaining a dynamic prediction of the simultaneous thermal comfort and exergy-based thermodynamic performance of DX AC systems, this study attempts to develop a suitable ANN model that can cover a wide range of operation conditions and disturbances, which is suitable for model predictive control (MPC) applications. In the literature, there is no study that simultaneously studies the dynamic prediction of exergy destruction and thermal comfort for a DX AC system while considering the dynamic cooling load and ambient temperature variation using the ANN method.

Given the limited capability of conventional vapor compression systems for dealing with latent heat load, the thermal comfort addressed in this paper is limited to the indoor air temperature only, while

the exergy destruction is used to evaluate the efficiency of the system. The inclusion of indoor humidity as a parameter for the system identification and predictive control could be more suitable when dealing with desiccant cycles or hybrid systems. The exergy analysis characterizes the energy dissipation rates in every component during dynamic operation. This enables the AC system to reach the target indoor temperature while operating at high thermodynamic performance. Accordingly, a novel ANN model that can be used to capture the dynamic behavior of the room temperature and exergy destruction under modulation of the compressor speed, dynamic cooling load, and ambient temperature is developed; the comparison between Bayesian regularization and the early stopping method, which is frequently used in the aforementioned studies, is presented. The Bayesian regularization approach is eventually applied to improve the generalization capability of the ANN model. Additionally, since model-based simulation data are used for the ANN training, these can be obtained for a large variety of system characteristics (working fluid, capacity, size, etc.) under the range of validity of the modeling assumptions.

2. System description

The main motivation of the present study is to develop an identification method for AC systems. To reduce the complexity, the data for the training and testing of the ANN method are generated with a dedicated simulation software that was previously presented and validated [27,28]. Accordingly, the details of the simulation platform are referred to in previous literature, and the description of a suitable experimental investigation and data acquisition method will be dealt with in a following study. The simulation software is developed using a C++ program containing mathematical models that describe the dynamic behavior of all components including the variable speed compressor (VSC) model, fin-tube heat exchangers used as a condenser and evaporator, electronic expansion valve (EEV), and room model. The thermodynamic properties of the refrigerant obtained from the REFPROP library are used when calculating the energy balance and heat transfer processes. The mathematical model of the compressor is developed by following two main assumptions: firstly, there is a stable loss of entropy and energy when the refrigerant is compressed; secondly, the refrigerant mass flow rate changes according to the compressor speed. The evaporator and condenser are modeled using a distributed parameters model where the variable heat transfer coefficient and pressure loss of the refrigerant flow are considered. The heat transfer coefficient calculation employs the Dittus-Boelter's equation [29] for the single-phase refrigerant condition, while Shun's [30] and Shigeru's [31] equations are adopted for the two-phase refrigerant during the evaporation and condensation processes, respectively. The refrigerant undergoes an isenthalpic process when passing through the expansion valve. Moreover, the pipelines that connect every component within the system are assumed to be perfectly insulated. Additionally, the effect of pressure loss in the pipelines is neglected because the pipe used to connect each component in a split A/C system is usually very short and could vary depending on the specific application [32].

The system schematic diagram is depicted in Fig. 1(a). Basically, the evaporator absorbs the heat, Q_E, from the conditioned space at the room air temperature, T_R [Eq. (1)]. Then, by increasing the refrigerant pressure using the compressor, the heat, Q_C, is released to the environment at temperature T_A. The inlet temperature on the air-side of the evaporator represents the room temperature affected by the building cooling load, while the outlet temperature is lowered by the evaporation process occurring on the refrigerant side. The numbers one to four in Fig. 1(b) are used to identify the fundamental states of the refrigerant dividing the single thermodynamic processes.

The dynamic response of the room temperature is calculated using the following equation:

$$\rho C_p V \frac{dT_R}{dt} = Q_E - Q_l \tag{1}$$

where ρ is the air density; C_p is the air heat capacity; and V is the air volume, which is equal to the room volume. Then Q_E and Q_l represent the cooling capacity and cooling load, respectively.

3. Thermodynamic analysis

In real applications, a vapor compression A/C system, as other operative cooling systems [33], deviates from the ideal inverse Carnot cycle owing to the irreversibility associated with the real and finite-time processes. First law-based efficiency analyses evaluate the output in terms of the cooling effect and compressor energy input only. This approach disregards the temperature levels of the heat sink and heat source, and does not characterize the energy losses in each component. Second law-based thermodynamic analyses provide a better understanding of the quality of each process with respect to their ideal counterparts (the corresponding reversible processes). Exergy analyses, which are based on the first and second laws of thermodynamics, are beneficial for investigating the energy potential loss in each component to improve the system operation. The basic exergy balance can be determined by [34]:

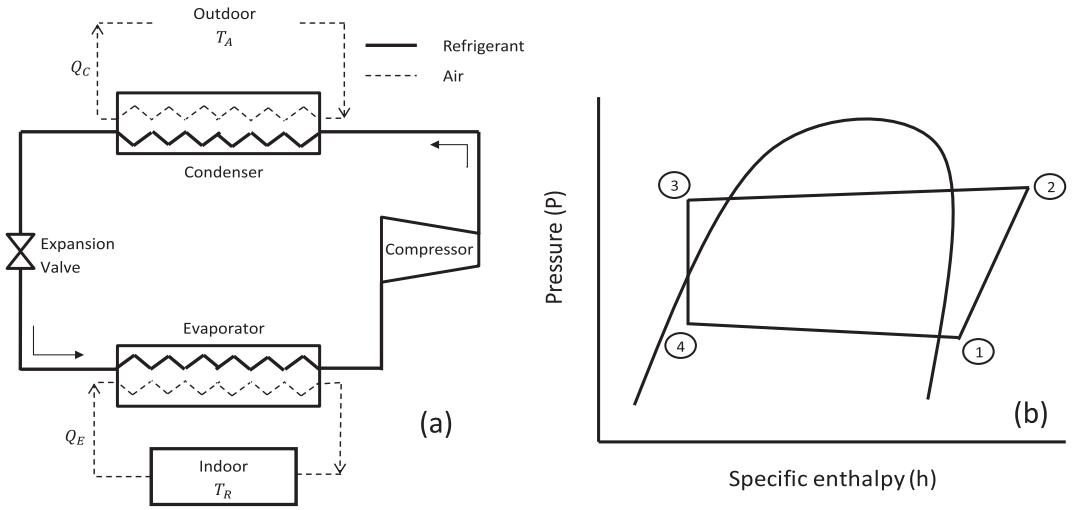

Fig. 1. (a) Vapor compression air conditioning system and (b) its p-h diagram.

$$\sum_{in}\left(1-\frac{T_0}{T_i}\right)Q+\dot{W}_{in}+\sum_{in}\dot{m}\dot{E}x = \sum_{out}\left(1-\frac{T_0}{T_i}\right)Q+\dot{W}_{out}+\sum_{out}\dot{m}\dot{E}x+\dot{E}x_{dest} \quad (2)$$

where $\dot{E}x$ is the specific exergy flow; the subscripts *in* and *out* represent the inlet and outlet, respectively; $\dot{m}$ is the mass flow rate; Q represents the heat transfer rate between the heat exchanger and its surrounding; $\dot{W}$ is the work rate; and $\dot{E}x_{dest}$ is the exergy destruction. $\left(\frac{T_0}{T_i}\right)$ indicates the temperature ratio of the dead state condition, T_0, with the heat exchanger surrounding, T_i. In this case, the temperature at the condenser surrounding is assumed to be the same as the ambient temperature.

The specific exergy flow at state m can be calculated by

$$\dot{E}x = [(h_m - h_0) - T_0(s_m - s_0)] \quad (3)$$

where h_0 and s_0 are the specific enthalpy and entropy, respectively, at the dead state temperature T_0, which is equal to the ambient temperature.

The simplified governing equations for the exergy analysis of all components are given by Eqs. (4)–(9) (for the state numbers refer to Fig. 1) [35].

Compressor

$$\dot{E}x_{dest,1-2} = \dot{m}T_0(s_2 - s_1) \quad (4)$$

Condenser

$$Q_C = \dot{m}(h_3 - h_2) \quad (5)$$

Expansion valve

$$\dot{E}x_{dest,3-4} = \dot{m}T_0(s_4 - s_3) \quad (6)$$

Evaporator

$$Q_E = \dot{m}(h_1 - h_4) \quad (7)$$

$$\dot{E}x_{dest,4-1} = T_0\dot{m}\left[(s_1 - s_4) + \frac{Q_E}{T_R}\right] \quad (8)$$

Finally, the total exergy destruction is determined by combining the exergy destruction of all components, and is expressed as follows:

$$\dot{E}x_{dest,total} = \dot{E}x_{dest,1-2} + \dot{E}x_{dest,2-3} + \dot{E}x_{dest,3-4} + \dot{E}x_{dest,4-1} \quad (9)$$

4. Artificial neural network design

4.1. Multi-layer perceptron structure

An ANN model with a multi-layer perceptron (MLP) configuration has been successfully applied for prediction purposes [36,37]. The simplified structure of the MLP-ANN, shown in Fig. 2, consists of input, hidden, and output layers. All signals from the input are connected to the neurons and transmitted to the output in one direction. There is at least one neuron in the hidden layer that builds up the connection between the input and output.

Mathematically, the predicted output generated from the MLP-ANN is given by:

$$y(k) = f_2(w_2 n(k) + b_2) \quad (10)$$

$$n(k) = f_1(w_1 u(k) + b_1) \quad (11)$$

where $u(k)$ and $y(k)$ are the input and output vectors, respectively. The state vector, which represents the output from the hidden layer is represented by $n(k)$. The correlation between the input and hidden layers is connected by the weight coefficient w_1. Meanwhile, the weight coefficient w_2 connects the hidden and output layers. The notation f_1 and f_2 represents the activation functions in the hidden and output layers, respectively. The parameters b_1 and b_2 are the bias coefficients in the hidden and output layers, respectively. Subsequently, a back-propagation algorithm is applied to train a network to adjust the weight and bias coefficients to minimize the error between the target and predicted outputs. A tangent sigmoid activation function [Eq. (12)] is used in the present study. One hidden layer is employed for the training because a large number of hidden layers increases the network size but does not significantly improve the accuracy [19]. The learning rate is set to 0.01 to keep the training speed high enough, while still achieving a high accuracy.

$$\tanh(n) = \frac{2}{1+e^{-2n}} - 1 \quad (12)$$

The architecture of the ANN model used in present study is demonstrated in Fig. 3. The instantaneous room temperature T_R and total exergy destruction Ex_{dest} at time t are predicted using the history of the compressor speed N, cooling load Q_L, ambient temperature T_A, and room temperature with the number of tapped delay lines (TDLs) represented by *du* and *dy*.

4.2. Bayesian regularization algorithm

Overfitting occurs when the network fits the training data too rigidly and provides a poor prediction accuracy when applied to new data. Network complexity is highly correlated with the generalization capability of the ANN model; a lower network complexity produces a better generalization. The larger the network size, the more complicated the set of built mathematical functions, and thus the network has higher complexity and a poor generalization capability [38]. The Bayesian regularization algorithm is considered as an ideal approach for solving the learning task of ANN [39]. The main principle of the Bayesian regularization method is the modification of the sum squared error performance index, performed by adding the sum of the squared weight that penalizes the network complexity [Eq. (13)]. The importance of adding the sum squared weight is to restrict the weight coefficient to a small number, and accordingly, the network function can generate a smooth interpolation through the training data. Therefore, overfitting can be avoided.

The regularization term can be expressed as follows:

$$J_{reg} = \beta E_D + \alpha E_W \quad (13)$$

where J_{reg} is an objective function to be minimized; E_D is the sum of the squared errors of the actual and predicted values; E_W is the sum squared error of the network weight; and α and β are the objective function parameters (regularization parameters).

The network complexity can be reduced by adjusting the ratio of α and β. If this ratio is properly determined, the regularization produces a network that generalizes the system behavior well. In a Bayesian network, the network weights are assumed to be random variables. The density function of the weights and ratio of α and β are then determined using Bayesian's theorem, which is described by the following equation:

$$P(x|D, \alpha, \beta, M) = \frac{P(D|x, \beta, M)P(x|\alpha, M)}{P(D|\alpha, \beta, M)} \quad (14)$$

where x is the vector containing the weight and bias in the network; D represents the datasets for training; and M is the designed network architecture. The details regarding the Bayesian regularization used for improving the generalization is further explained in Ref. [38].

The network complexity is determined by summing all of the weight

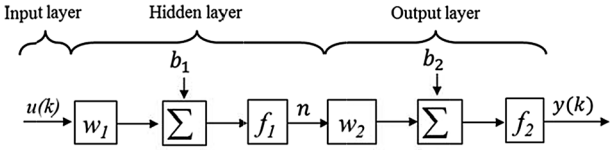

Fig. 2. Multilayer perceptron network.

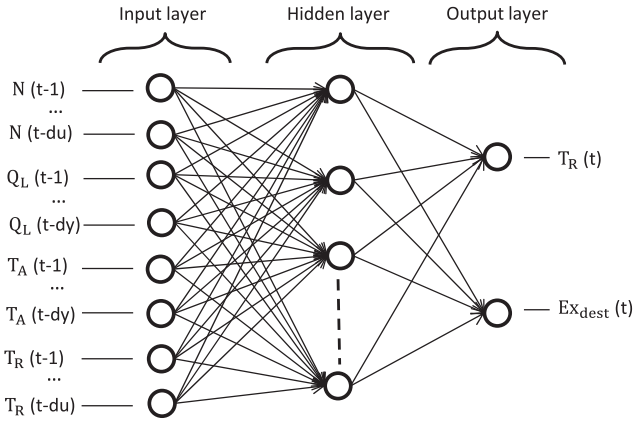

Fig. 3. Dynamic ANN architecture.

and bias coefficients required to fit the data [41]. In Eq. (15), the coefficients c_1 and c_2 are the weighting factors used to emphasize the contribution of the weight and bias coefficients to the network complexity. Since the size of the weight matrix is larger than the bias matrix, in the present study the ratio of c_1 and c_2 is set to 10, indicating that the influence of the weight coefficients is more significant than that of the bias coefficients.

$$Net_{comp} = c_1 \sum_{1}^{k} (w_{1,k} + w_{2,k}) + c_2 \sum_{1}^{k} (b_{1,k} + b_{2,k}) \tag{15}$$

During the training process the bias and weight coefficients are optimized to minimize the objective function in Eq. (13). The training is stopped when one of the following convergence criterions is reached:

- Epoch (number of iteration): 1000
- Error threshold: 0

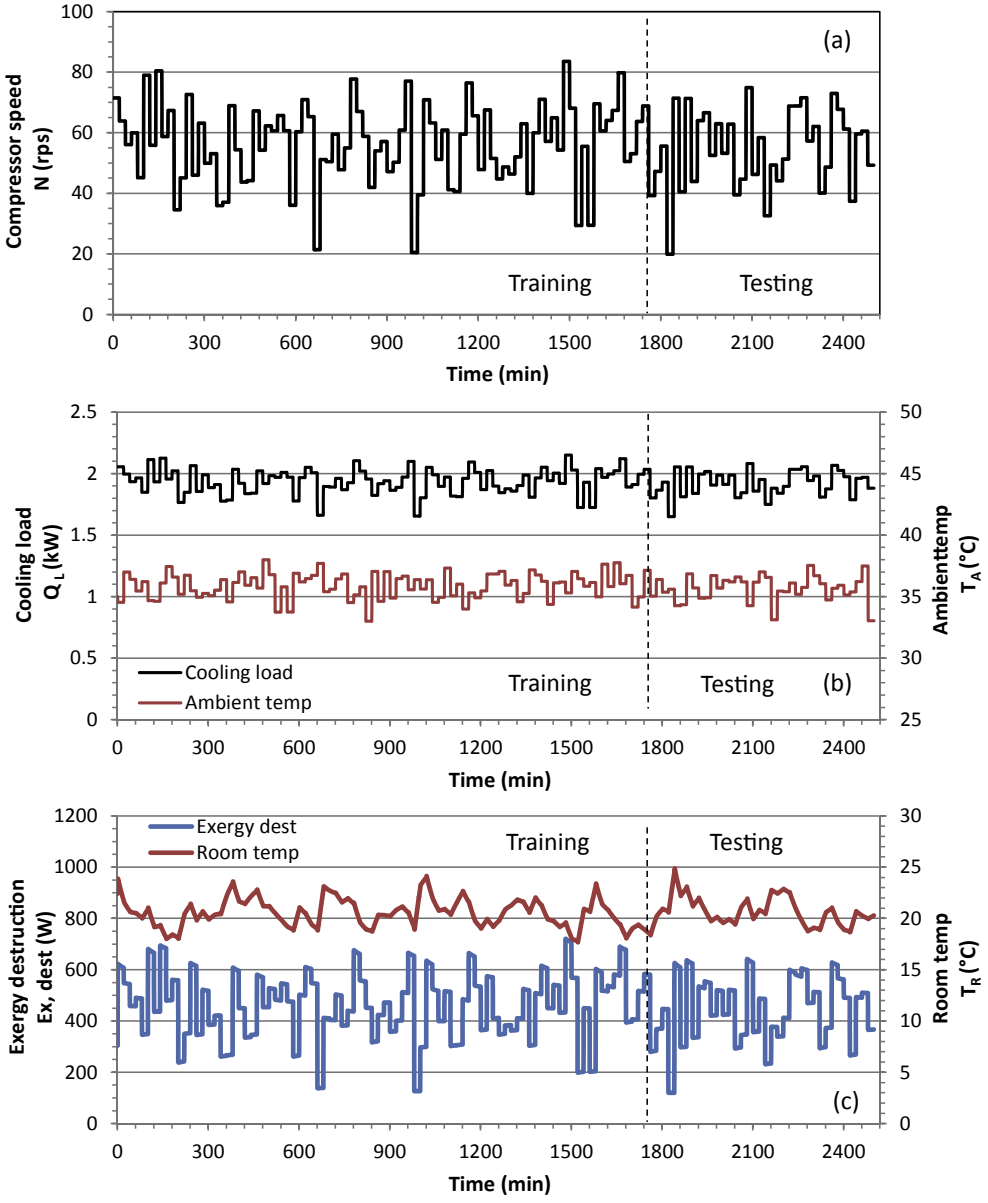

Fig. 4. Input-output data used for the training and testing of the ANN: (a) system input (compressor speed); (b) disturbance input (cooling load and ambient temperature); and (c) system output (exergy destruction and room temperature).

- Performance gradient (J_{reg}): 10^{-7}

The error metrics of RMSE, CV, and absolute error are used to measure the prediction accuracy. The the RMSE value [Eq. (16)] illustrates how well the data are fitted, and the CV value [Eq. (17)] indicates the percentage of the average error compared with the average of the corresponding data. The absolute error [Eq. (18)] quantifies the prediction error for every single data point.

$$\mathrm{RMSE} = \sqrt{\frac{1}{P}\sum_{j=1}^{P}(y_j - t_j)^2} \tag{16}$$

$$\mathrm{CV} = \frac{RMSE}{\frac{1}{P}\sum_{j=1}^{P} y_j} x100 \tag{17}$$

$$\mathrm{Absoluteerror} = |y_j - t_j| \tag{18}$$

Here, y_j and t_j are the predicted and calculated values, respectively, and P represents the total number of data points.

4.3. Simple additive weighting

The multi criteria decision making method using simple additive weighting (SAW) is applied to select the optimum ANN model while considering the network complexity and prediction accuracy of the room temperature and exergy destruction. In this method, the accuracy of the room temperature (RMSE, T_R) is selected as the first preference criterion because this parameter is the main controlled objective. The second preference criterion is the accuracy of the exergy destruction (RMSE, Ex_{dest}), followed by the network complexity (Net_{comp}).

The decision making process begins with the initialization of the weight for each attribute, w_j, based on the aforementioned preference criteria. The attribute score is then normalized by the following equation

$$r_{ij} = \frac{Minx_{ij}}{x_{ij}};\ i = 1, 2, \cdots, n_a;\ j = 1, 2, \cdots, n_p \tag{19}$$

where n_a represents the number of alternatives that contain the various ANN models; n_p is the number of attribute/performance criteria; r_{ij} is the normalized score from an alternative A_i on attribute C_j.

The preference value for each alternative (V_i) is determined by

$$V_i = \sum_{j=1}^{n_p} w_j r_{ij} \tag{20}$$

A lower V_i indicates a better ANN model because the ANN model with a low RMSE and network complexity is desired.

5. Simulation design

The purpose of the simulation is to provide sufficient information regarding the dynamic behavior of the AC system in a wide operating range. In this work, the system is operated under the modulation of the compressor speed, cooling load, and ambient temperature to obtain the dynamic response of the room temperature and total exergy destruction. The n-sample-constant method is selected for the signal excitation of the compressor speed, which is well suited for dynamic system identification [40]. As it covers various amplitudes in a wide range, this signal contains the appropriate pattern for introducing the dynamics of the system.

The system is simulated by varying the compressor speed between 19.8 and 83.5 rps with the hold time set at 20 min, which is close to the time constant determined by the step response test. The hold time should not be too short or too long. A short hold time leads to a system with insufficient time to settle down. On the other hand, if the hold time is too large, data redundancy will exist at the steady state condition [41]. The ambient temperature and cooling load is changed every 20 min from 30 to 37 °C and 1.7–2.3 kW, respectively, with the assumption that there is no significant change in the ambient temperature and cooling load within 20 min. In the real condition, the ambient temperature changes smoothly, and the cooling load in the residential building fluctuates in low frequency. To achieve a more precise prediction accuracy, the ambient temperature and cooling load pattern can be obtained from the actual building and location where the ANN model will be applied. It is important to note that during the data generation for the ANN training, the superheat temperature is maintained at 5 °C by the PI controller, and a constant fan speed is set for the evaporator and condenser. In control application, the developed ANN model is applied together with the PI controller to control the room and superheat temperatures, while minimizing the exergy destruction by regulating the compressor speed and valve opening with constant air flow rates in the evaporator and condenser [42].

Since the ANN model is developed for predictive control purposes, the manipulated parameter (compressor speed) and disturbances (cooling load and ambient temperature) are included in the set of input parameters of the model. As shown in Eq. (1), the dynamic room temperature response is strongly affected by the system operation, cooling load, and conditioned room volume. To include the effect of all of these parameters, the room temperature with a certain time delay is used as an input to achieve an accurate prediction.

In total, there are 5000 pairs of input and output data from the simulation; the first 3500 data pairs are used for training to generate the network, and the last 1500 data pairs are used for testing. The input and output data pattern used for the system identification is shown in Fig. 4. This demonstrates the response of the total exergy destruction and room temperature under modulation of the compressor speed and by including the influence of the cooling load and ambient temperature with a sampling time of 30 s. The trend of the total exergy destruction is similar to the compressor speed signal in the same frequency range. This is due to the change of the compressor speed leading to changes in the refrigerant mass flow rate and pressure, and these two parameters have a strong influence on the exergy destruction. Thus, the exergy destruction results are very sensitive to compressor speed fluctuations. Conversely, the response of the room temperature with respect to the compressor speed is very slow. This is caused by the effect of the cooling load, ambient temperature, room size, and cooling effect supplied by the system, which produces a time delay of the temperature response.

Table 1
Comparison of the early stopping (ES) and Bayesian regularization (BR) under various numbers of neurons.

Number of neurons	RMSE of Ex, dest (W)		RMSE of T_R (°C)		CV of Ex, dest (%)		CV of T_R (%)		Network complexity	
	ES	BR	ES	BR	ES	BR	ES	BR	ES	BR
1	2.67	2.67	1.29	1.29	0.60	0.60	6.23	6.24	14.40	14.26
3	1.84	1.56	0.35	0.08	0.42	0.35	1.68	0.37	2208.42	5.03
5	1.52	1.40	0.18	0.14	0.34	0.32	0.85	0.69	58.33	163.25
7	1.67	1.80	0.25	0.13	0.38	0.41	1.22	0.65	586.03	214.12
9	1.28	1.41	0.27	0.09	0.29	0.32	1.29	0.45	813.69	122.82
11	1.86	1.46	0.20	0.05	0.42	0.33	0.98	0.26	152.65	99.88

Table 2
Comparison of early stopping (ES) and Bayesian regularization (BR) under various numbers of time delay lines (TDLs).

Number of TDLs		RMSE of Ex, dest (W)		RMSE of T_R (°C)		CV of Ex, dest (%)		CV of T_R (%)		Network complexity	
du	dy	ES	BR	ES	BR	ES	BR	ES	BR	ES	BR
2	2	1.92	5.60	0.12	0.10	0.44	1.27	0.56	0.47	128.04	126.80
3	3	1.65	5.99	0.18	0.08	0.37	1.36	0.85	0.40	379.02	226.67
4	4	1.54	5.83	0.12	0.05	0.35	1.32	0.57	0.23	312.59	192.75
5	5	2.04	3.85	0.17	0.05	0.46	0.87	0.81	0.26	383.09	281.93
6	6	2.11	5.80	0.11	0.05	0.48	1.31	0.55	0.27	86.22	219.73
7	7	1.58	5.82	0.21	0.05	0.36	1.32	1.03	0.23	160.97	290.61

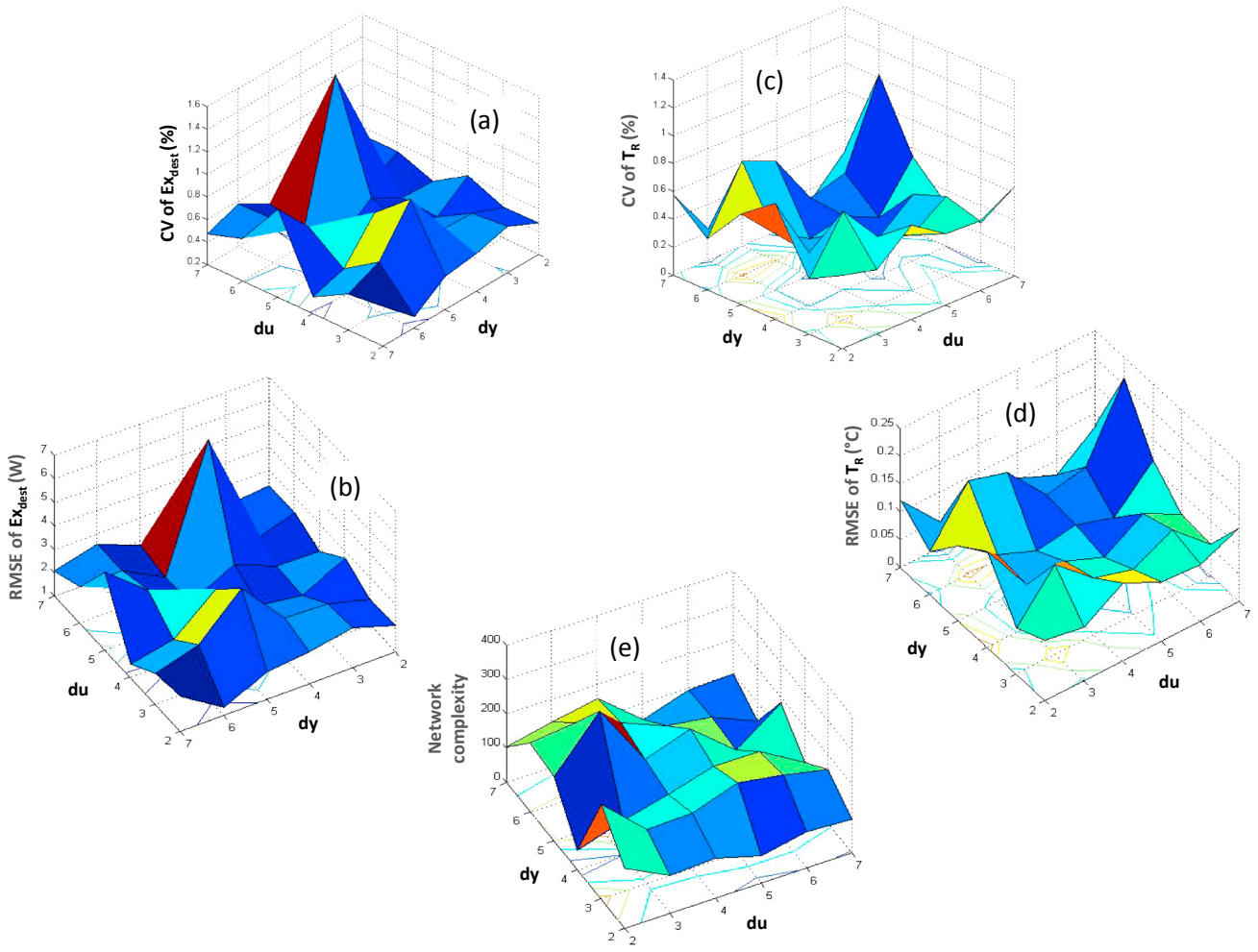

Fig. 5. Effect of the number of time delay lines on the: (a, b) exergy destruction prediction; (c, d) room temperature prediction; and (e) network complexity.

6. Results and discussion

The results of the ANN development for system identification, including its validation are presented in this section. For the ANN development, the prediction accuracy obtained from the testing data is considered as the reference that indicates the actual performance of the ANN model. Thus, the ANN performance is measured by the error when the network is applied in the testing data, which is never used in the training phase. There is no exact rule for obtaining the optimized ANN configuration with global optima results. Since there are many parameters that affect the prediction accuracy, such as the learning rate, optimization method, number of inputs, number of time delays, and network structure, these need to be fixed prior to performing the global optimization procedures [43]. As a consequence, the weight and bias coefficients generated by the convergence of training process will change in relation to all of these parameters, and therefore the reached global optimum might not actually be a global optimum for the network. Hence, the number of time delays and neurons are optimized separately as in Ref. [41].

6.1. Generalization capability

In previous studies, the early stopping method has been frequently applied to generalize the network. Nonetheless, this method tends to produce overfitting when applied to new data due to improper time decision criterion that stops the network training. Hence, Bayesian regularization is hereby proposed to achieve high generalization features in the ANN training. A comparison of the early stopping and Bayesian generalization approach is performed by investigating the prediction accuracy and network complexity for various numbers of

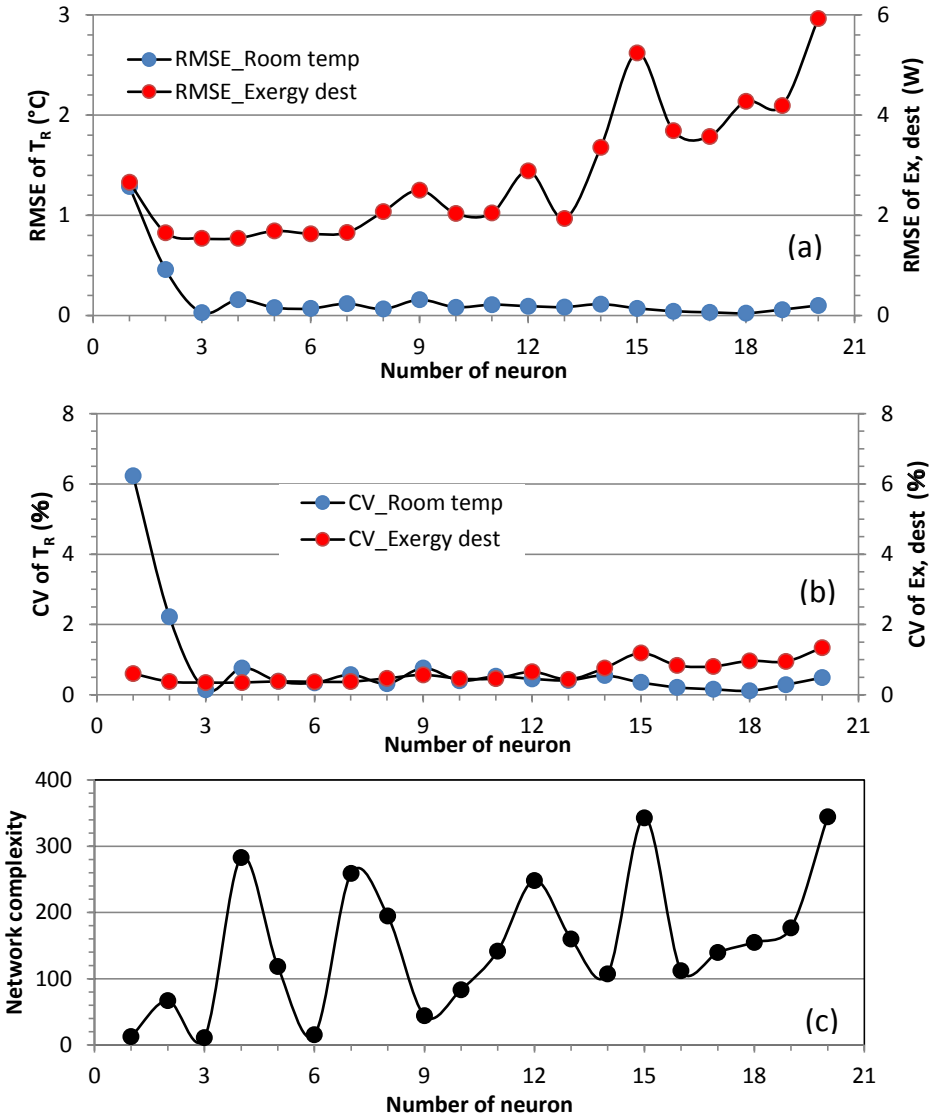

Fig. 6. Effect of the number of neurons on the prediction accuracy: (a) RMSE, (b) CV, and (c) network complexity.

Table 3
Final ANN architecture.

Network properties	Network architecture
Number of time delay lines	du = 5 and dy = 6
Number of neurons	3
Generalization method	Bayesian regularization
Error threshold	0
Max number of iterations	1000
Learning rate	0.01
Number of hidden layers	1
Transfer function	Tangent sigmoid

neurons (Table 1) and TDLs (Table 2).

Table 1 indicates that the accuracy of the Bayesian regularization is generally better than that of early stopping for the prediction of the exergy destruction and room temperature. For the structures with only seven and nine neurons, early stopping provided a marginally better accuracy in predicting the exergy destruction. The highest difference in the RMSE (0.27 °C and 0.28 W) and network complexity (438%) is shown for the case with three neurons. Moreover, the network complexity obtained by early stopping is mostly higher for all ANN models, except for five neurons. As the number of neurons increase, the network complexity performed by early stopping fluctuates with a deviation of 759. For the Bayesian regularization, the network complexity can be successfully minimized below 215 with a deviation of 75.11. These results demonstrate that the Bayesian regularization is able to maintain a low network complexity without sacrificing the prediction accuracy.

A comparison of early stopping and Bayesian regularization under various numbers of TDLs is summarized in Table 2. This shows that the early stopping case is better at predicting the exergy destruction, compared with Bayesian regularization, with an average relative error of 32.9%. On the other hand, the room temperature predictions are more accurate for Bayesian regularization, with an average relative error of 41.7%. The highest RMSE difference for the exergy destruction (4.34 W) for three TDLs is not significant when compared to the corresponding data, which ranges from 119.19 to 652.18 W. Meanwhile, the highest RMSE difference for a temperature of 0.16 °C for seven TDLs is less marginal as the room temperature varies from 18.35 to 24.87 °C. Therefore, the accuracy of the room temperature is prioritized in the present work. Accordingly, Bayesian regularization is preferred for applications of the present study.

The ANN training using early stopping may have good accuracy and low network complexity due to a proper stopping decision. However, since the initial weight coefficient is randomly set, and the objective function only contains the sum squared error, it is hard to achieve a

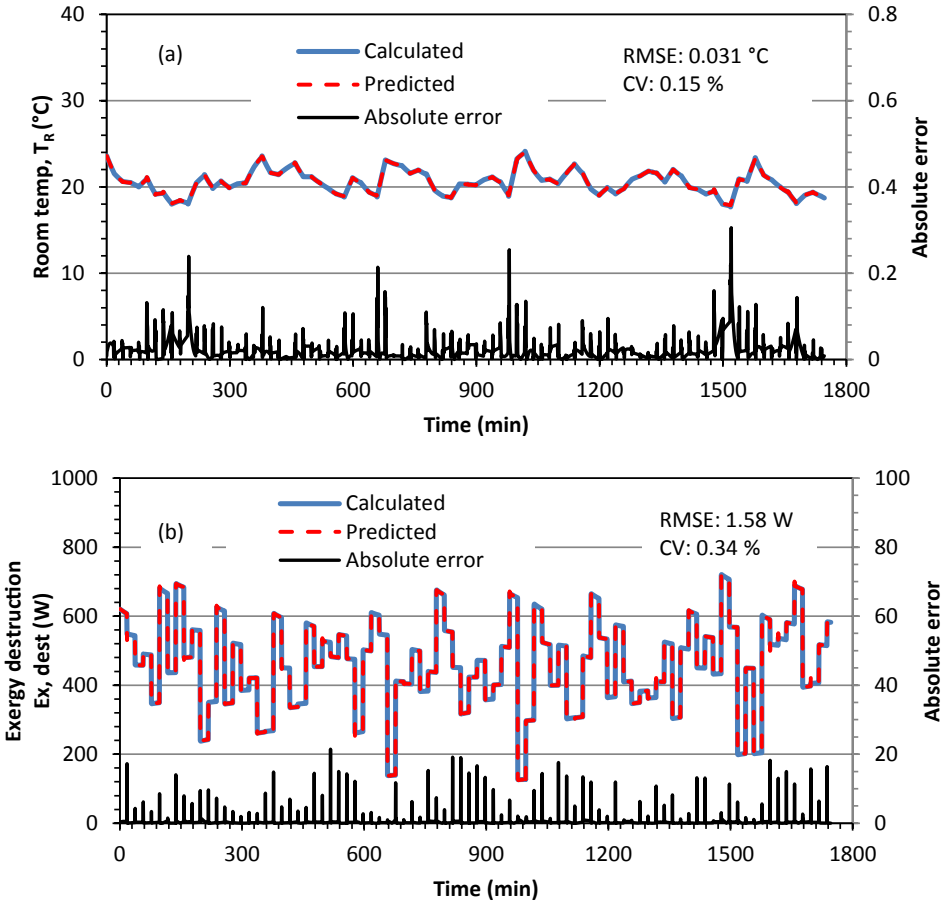

Fig. 7. Training results for the (a) room temperature and (b) exergy destruction.

high accuracy and generalization capability simultaneously using the early stopping method.

Practically, when early stopping is performed, ANN is trained by dividing the available data into two groups intended for training and validation. The datasets for validation are used to determine how well the network is performing. Then, the training is terminated once the error in the validation data increases after several iterations. Consequently, it does not guarantee that the trained network has reached the minimum error and has small weight coefficients. On the other hand, the ANN model with Bayesian regularization trains the network to simultaneously minimize the prediction error and network complexity. The network training is stopped when it reaches one of the convergence criteria provided in the previous section. The objective function, which consists of the sum-squared error and sum-squared weight, should reach constant values when the network has converged. Therefore, the training with Bayesian regularization can ensure that the network has a high generalization capability, while maintaining a small prediction error.

6.2. Optimal number of tapped delay lines

In this section, the influence of the input and output history, which represents the relationship between the current outputs (exergy destruction and room temperature) and previous compressor speed, cooling load, and ambient temperature, is investigated. The input delay is applied to the compressor speed and room temperature, which is denoted by *du*, and the cooling load and ambient temperature are expressed by *dy*. As the room temperature is easy to measure during real time operation, this parameter is included as the feedback input. Meanwhile, the input history of the exergy destruction is not considered because of its measurement complexity.

Fig. 5 demonstrates the effect of the number of TDLs on the prediction accuracy and network complexity. The number of TDLs is incrementally increased to two, three, four, five, six, and seven, which generates 36 different network models with various *du* and *dy* combinations. In this case, all ANN models are trained with ten neurons and Bayesian regularization, then the error and network complexity results are plotted in a 3D graph. Using the graphs, various combinations of *du* and *dy* lead to the prediction accuracy and network complexity changes. If low numbers of TDLs are applied, it is difficult for the network to capture the system dynamic due to insufficient information regarding the previous states recorded in the network. Otherwise, if too many input delays are included, the network will be very sensitive to the training data and produce overfitting. Moreover, the number of TDLs has a strong influence on the network complexity.

The optimal number of TDLs is determined by the 3D graph shown in Fig. 5. The optimal network is selected by the simple adaptive weighting (SAW) method with the room temperature accuracy is considered as the first preference criteria, followed by the exergy destruction accuracy and network complexity. Accordingly, the network structure with five *du* (time delay of the compressor speed and room temperature) and six *dy* (time delay of the cooling load and ambient temperature) can be selected as the optimal structure, since this ANN model yields a good prediction accuracy along with low network complexity.

6.3. Optimal number of neurons

In this section, the optimal number of neurons is also selected by considering the network complexity and prediction accuracy. Fig. 6

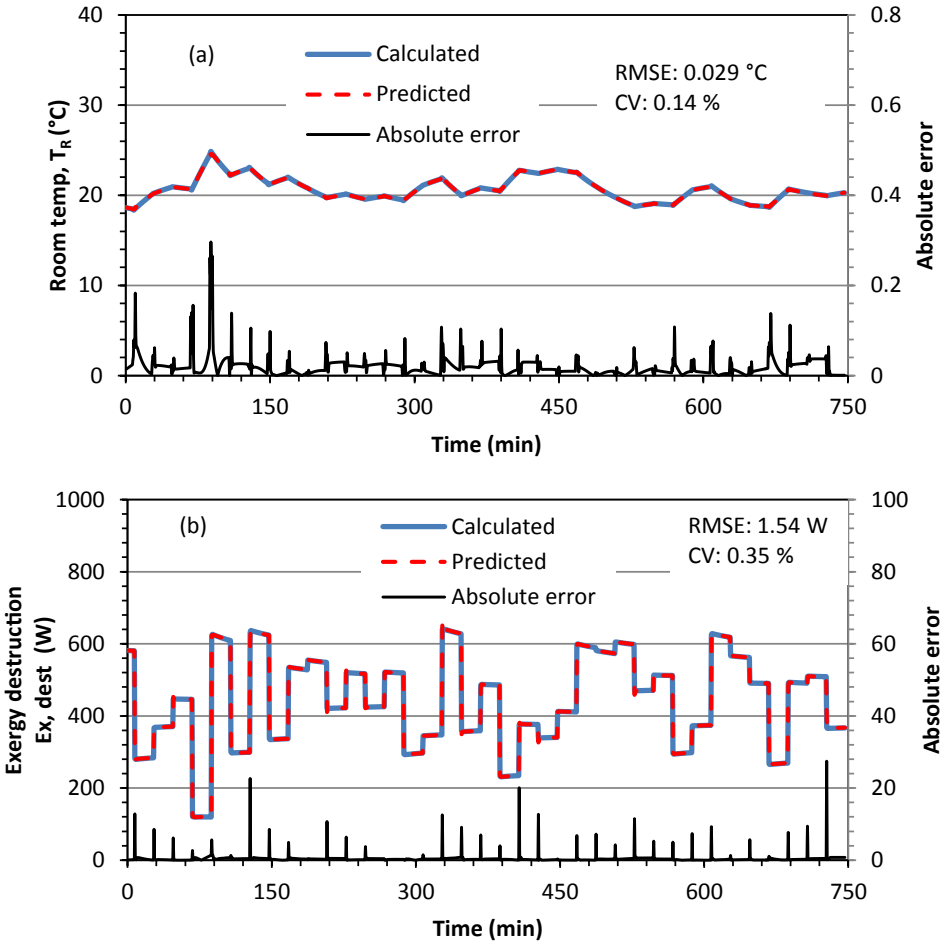

Fig. 8. Validation results of the one-step ahead prediction: (a) room temperature and (b) exergy destruction.

demonstrates the effect of the number of neurons on the prediction accuracy and network complexity. The network is trained by varying the number of neurons from 1 to 20 in the hidden layer. The other network parameters are set to be equal to the previously selected values (five TDLs at *du* and six TDLs at *dy*). The accuracy metrics of RMSE and CV shows the similar trend. Initially, the prediction error decreases as the number of neurons increases. Then, stable and accurate results for the room temperature and exergy destruction are obtained after three to seven neurons where the RMSE values can be maintained within small values. Furthermore, the prediction accuracy of the exergy destruction worsens after eight neurons. When only a few neurons are applied during training, the network is not flexible and has an inadequate number of weights to simultaneously minimize the network complexity and prediction error. Conversely, a higher number of neurons will result in a higher network size, which potentially increases the network complexity. Based on the results presented in Fig. 6, among the ANN models with three to seven neurons, the ANN structure using three neurons has the lowest network complexity. This ANN model is considered as the optimum model.

6.4. Network validation

The optimal ANN configuration for the system identification has been developed in the previous section by considering the network complexity, generalization capability, and prediction accuracy. The fundamental features of the optimized ANN model are listed in Table 3.

The training result of the developed ANN is shown in Fig. 7. A comparison of the predicted and corresponding values for the room temperature and exergy destruction are depicted in Fig. 7(a) and 7(b), respectively. The training accuracy for the temperature yields RMSE of 0.031 °C, CV of 0.15%, and maximum absolute error of 0.3 °C. Furthermore, for the exergy destruction predictions, RMSE of 1.58 W, CV of 0.34%, and a maximum absolute error less than 22 W are obtained. These error indicators show that the developed ANN model has precisely fitted the data.

In practice, the testing accuracy is more important than the training accuracy because an accurate prediction in the training phase does not automatically imply that the network has a good prediction capability. The network performance should be validated to predict other data that are not introduced beforehand. The validation results for the one-step-ahead prediction of the room temperature and exergy destruction are shown in Fig. 8(a) and 8(b), respectively. The validation results for the room temperature demonstrate a good agreement between the predicted and corresponding values with RMSE of 0.029 °C, CV of 0.14%, and a maximum absolute error less than 0.3 °C. Additionally, the validation results for the exergy destruction also demonstrate a good prediction accuracy with RMSE of 1.54 W, CV of 0.35%, and an absolute error less than 28 W. According to this result, the difference between the accuracies for the training and testing results is not significant. -This indicates that the developed ANN model with Bayesian regularization has a strong generalization capability and good accuracy.

To ensure that the ANN model can be applied for predictive control, the validation of the multi-step-ahead prediction is presented. The difference between the one- and multi-step-ahead predictions is the source of the past temperature value. The past room temperature is required to use as input in both the one- and multi-step-ahead predictions. Multi-step-ahead prediction is suitable for application cases where the direct measurement of the room temperature is not available,

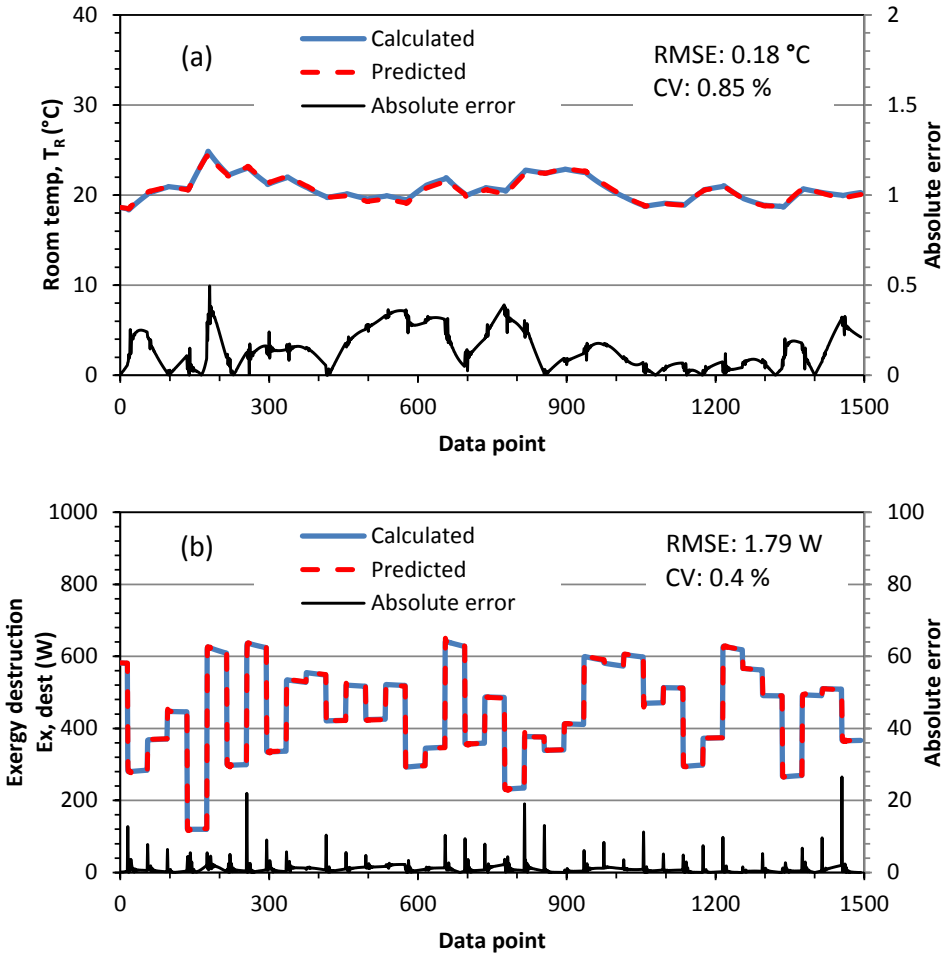

Fig. 9. Validation result of the multi-step-ahead prediction: (a) room temperature and (b) exergy destruction.

alternatively the predicted room temperature from the ANN is fed back as the input to predict the next output. If the actual temperature can be directly measured, a one-step-ahead prediction can be used, which is covered in detail in Ref. [41].

Fig. 9 demonstrates the validation results of the multi-step-ahead prediction for the room temperature and exergy destruction. The developed ANN model is tested to predict 1493 steps of the room temperature and exergy destruction to evaluate the ANN performance capability when applied to various amplitudes of the variations without external temperature inputs. When applied to the predictive control, only few steps ahead predicted data are used to avoid a high computational task during the online optimization. Based on Fig. 9(a), the predicted temperature is in good agreement with the corresponding value. From these results the RMSE value is 0.18 °C, CV is 0.85%, and maximum absolute error is less than 0.5 °C. A comparison of the predicted and calculated values of the exergy destruction is provided in Fig. 9 (b). The results yield RMSE value of 1.79 W, CV of 0.4%, and a maximum absolute error of 26.5 W.

A comparison of the validation results of the one- and multi-step-ahead predictions (Figs. 8 and 9, respectively), shows that the one-step-ahead prediction has a better accuracy since the past value is taken from the true value. Nonetheless, the validation results generated by the multi-step-ahead prediction indicate a good accuracy with RMSE of 0.18 °C for the room temperature; this error is still acceptable for the room temperature prediction. Meanwhile, RMSE of 1.79 W for the exergy destruction indicates an excellent accuracy since the range of exergy destruction is between 119.84 and 720.42 W. According to this result, the developed ANN provides a good performance for the multi-step-ahead prediction and its application to predictive control is feasible. Nonetheless, when the ANN models are applied to actual systems, the training data obtained from the measured data in the experimental system are affected by the steady state and dynamic uncertainties. Therefore, the data should be properly selected while considering the noise, outliers, and frequency [40]. This step is necessary to enable the ANN model to achieve an appropriate characterization of the dynamic behavior of the system. To develop an exergy based optimal control using a single actuator, provided that these issues are properly addressed, the compressor speed can be optimized to minimize a combined objective function that simultaneously considers deviations from the set indoor temperature and exergy destruction (see for example Ref. [44], where a weighting factor is assigned to each term of the objective function to achieve a reasonable reference tracking performance).

7. Conclusion

A back-propagation ANN model has been developed for the system identification of a single (actuator) input and multiple outputs of a DX AC system. The dynamic response of the room temperature and exergy destruction is predicted with respect to the modulation of the compressor speed, dynamic cooling load, and ambient temperature. The ANN model is comprehensively optimized by considering the generalization capability, network complexity, number of neurons, and optimal tapped delay lines. For the ANN training, the Bayesian regularization approach has successfully minimized the network complexity to ensure a high generalization of the ANN without sacrificing the prediction accuracy. The optimized ANN model with three-neurons; five-delayed inputs for the compressor speed and room temperature; six-

delayed inputs for the cooling load and ambient temperature; and the Bayesian regularization approach demonstrated a good prediction capability when applied to either the one- or multi-step-ahead predictions with satisfying results. The validation of the multi-step-ahead prediction provided satisfying results with respect to the RMSEs and CVs of the room temperature (RSME: 0.18 °C and CV: 0.85%) and exergy destruction (RMSE: 1.79 W and CV: 0.4%). The results demonstrated that the ANN can be considered as an effective and efficient technique for system identification and used for multi-objective predictive control applications with a single actuator.

Acknowledgment

The author would like to thank LPDP (Indonesia Endowment Fund for Education) that has provided a scholarship to fund doctoral course and supported this research.

Appendix A. Supplementary material

Supplementary data to this article can be found online at https://doi.org/10.1016/j.applthermaleng.2019.113809.

References

[1] Nasruddin, et al., Potential of geothermal energy for electricity generation in Indonesia: a review, Renew. Sustain. Energy Rev. 53 (2016) 733–740.
[2] E. Council, Directive 2010/31/EU of the European Parliament and of the Council of 19 May 2010 on the energy performance of buildings, Off. J. Eur. Union 18 (201) (2010) 13–35.
[3] R.B. Jemaa, et al., Energy and exergy investigation of R1234ze as R134a replacement in vapor compression chillers, Int. J. Hydrogen Energy 42 (2017) 12877–12887.
[4] A. Lubis, et al., Experimental performance of a double-lift absorption heat transformer for manufacturing-process steam generation, Energy Convers. Manage. 148 (2017) 267–278.
[5] A. Lubis, et al., Solar-assisted single-double-effect absorption chiller for use in Asian tropical climates, Renew. Energy 148 (2016) 267–278.
[6] N. Giannetti, et al., Thermodynamic analysis of irreversible heat-transformers, Makara J. Technol. 19 (2015) 90–96.
[7] A. Milazzo, Future perspectives in ejector refrigeration, Appl. Therm. Eng. 121 (2017) 344–350.
[8] N. Giannetti, A. Milazzo, Thermodynamic analysis of regenerated air-cycle refrigeration in high and low pressure configuration, Int. J. Refrig. 40 (2014) 97–110.
[9] N. Giannetti, et al., Cascade refrigeration system with inverse Brayton cycle on the cold side, Appl. Therm. Eng. 127 (2017) 986–995.
[10] K. Ohno, et al., Performance evaluation method of heat pump driven refrigerated display cabinets, Refrig. Sci. Technol. (2018) 986–995.
[11] N. Li, et al., On-line adaptive control of a direct expansion air conditioning system using artificial neural network, Appl. Therm. Eng. 53 (1) (2013) 96–107.
[12] N. Jain, A. Alleyne, Exergy-based optimal control of a vapor compression system, Energy Convers. Manage. 92 (2015) 353–365.
[13] Q. Qi, S. Deng, Multivariable control of indoor air temperature and humidity in a direct expansion (DX) air conditioning (A/C) system, Build. Environ. 44 (8) (2009) 1659–1667.
[14] H. Pangborn, A.G. Alleyne, N. Wu, A comparison between finite volume and switched moving boundary approaches for dynamic vapor compression system modeling, Int. J. Refrig. 53 (2015) 101–114.
[15] Y. Yao, W. Wang, M. Huang, A state-space dynamic model for vapor compression refrigeration system based on moving-boundary formulation, Int. J. Refrig. 60 (2015) 174–189.
[16] A. Afram, et al., Artificial neural network (ANN) based model predictive control (MPC) and optimization of HVAC systems: a state of the art review and case study of a residential HVAC system, Energy Build. 141 (2017) 96–113.
[17] Q. Yang, et al., Simultaneous control of indoor air temperature and humidity for a chilled water based air conditioning system using neural networks, Energy Build. 110 (2016) 159–169.
[18] Nasruddin, et al., Solar absorption chiller performance prediction based on the selection of principal component analysis, Case Studies Therm. Eng. 13 (2019) 100391.
[19] Z. Tian, et al., Electric vehicle air conditioning system performance prediction based on artificial neural network, Appl. Therm. Eng. 89 (2015) 101–114.
[20] H.M. Kamar, et al., Artificial neural networks for automotive air-conditioning systems performance prediction, Appl. Therm. Eng. 50 (1) (2013) 63–70.
[21] F. Muñoz, et al., Real-time neural inverse optimal control for indoor air temperature and humidity in a direct expansion (DX) air conditioning (A/C) system, Int. J. Refrig. 79 (2017) 196–206.
[22] O. Rezayan, A. Behbahaninia, Thermoeconomic optimization and exergy analysis of CO2/NH3 cascade refrigeration systems, Energy 36 (2) (2011) 888–895.
[23] Nasruddin, et al., Optimization of a cascade refrigeration system using refrigerant C 3 H 8 in high temperature circuits (HTC) and a mixture of C2H6/CO2 in low temperature circuits (LTC), Appl. Therm. Eng. 104 (2016) 96–103.
[24] R. Prabakaran, D. Mohan Lal, A novel exergy based charge optimisation for a mobile air conditioning system, J. Therm. Anal. Calorim. 132 (2) (2018) 1241–1252.
[25] J.M. Belman-Flores, et al., Exergy assessment of a refrigeration plant using computational intelligence based on hybrid learning methods, Int. J. Refrig. 88 (2018) 35–44.
[26] R. Ben Jemaa, et al., Energy and exergy investigation of R1234ze as R134a replacement in vapor compression chillers, Int. J. Hydrogen Energy 42 (17) (2017) 12877–12887.
[27] K. Matsumoto, et al., Numerical analysis of VRF compression heat-pump system under unsteady-state condition, Trans. JSRAE 33 (2) (2016) 155–164.
[28] K. Saito, K. Ohno, Performance analysis of lower GWP refrigerants for air-conditioning systems using Energy flow + M, JRAIA Int. Symposium (2018).
[29] J.P. Holman, Heat Transfer (10th edition), McGraw-Hill, New York, 2010.
[30] Y. Shun, N. Kaneyasu, M. Takashi, N. Haruo, A study of heat transfer of refrigerant in a horizontal evaporating tube, Refrigeration 58 (666) (1983) 331–338.
[31] N. Shigeru, H. Hiroshi, H. Satoru, Superheated vapor condensation in a horizontal tube –suggestion of heat transfer and pressure equation, Refrigeration 58 (669) (1983) 659–668.
[32] M.J. Moran, H.N. Shapiro, Fundamentals of Engineering Thermodynamics, SI version, fifth ed.
[33] N. Giannetti, A. Rocchetti, K. Saito, Thermodynamic optimization of three-thermal irreversible systems, Int. J. Heat Technol. 34 (2016) S83–S90.
[34] N. Bouaziz, D. Lounissi, Energy and exergy investigation of a novel double effect hybrid absorption refrigeration system for solar cooling, Int. J. Hydrogen Energy 40 (39) (2015) 13849–13856.
[35] I. Dinçer, M. Kanoglu, Refrigeration Systems and Applications, second ed., John Wiley & Sons, Ltd, 2010 ISBN: 978-0-470-74740-7.
[36] S. Sholahudin, H. Han, Heating load predictions using the static neural networks method, Int. J. Technol. 6 (6) (2015) 946–953.
[37] S. Sholahudin, H. Han, Simplified dynamic neural network model to predict heating load of a building using Taguchi method, Energy 115 (2016) 1672–1678.
[38] M.T. Hagan, Neural Network Design, second ed., eBook, 2014.
[39] B. Heydecker, J. Wu, Identification of sites for road accident remedial work by Bayesian statistical methods: an example of uncertain inference, Adv. Eng. Softw. 32 (1011) (2001) 859–869.
[40] M. Norgaard, et al., Neural Networks for Modelling and Control of Dynamic Systems, Springer, 2001.
[41] B.C. Ng, et al., Dynamic modelling of an automotive variable speed air conditioning system using nonlinear autoregressive exogenous neural networks, Appl. Therm. Eng. 73 (1) (2014) 1255–1269.
[42] Jin-Long Lin, T.-J. Yeh, Modeling identification and control of air-conditioning systems, Int. J. Refrig. 30 (2007) 209–220.
[43] M. Mohanraj, et al., Applications of artificial neural networks for refrigeration, air-conditioning and heat pump systems—a review, Renew. Sustain. Energy Rev. 16 (2012) 1340–1358.
[44] N. Jain, G. Alleyne, Thermodynamics-based optimization and control of vapor-compression cycle operation: optimization criteria, American Control Conference on O'Farrel Street, (2011).